

Chemfire : a zone model for predicting chemical effects of pool fire in a single forced ventilation enclosure

Sylvain Brohez, Christian Delvosalle, Guy Marlair

▶ **To cite this version:**

Sylvain Brohez, Christian Delvosalle, Guy Marlair. Chemfire : a zone model for predicting chemical effects of pool fire in a single forced ventilation enclosure. 4. Mediterranean combustion Symposium, Oct 2005, Lisbonne, Portugal. pp.NC. ineris-00972509

HAL Id: ineris-00972509

https://ineris.hal.science/ineris-00972509

Submitted on 3 Apr 2014

HAL is a multi-disciplinary open access archive for the deposit and dissemination of scientific research documents, whether they are published or not. The documents may come from teaching and research institutions in France or abroad, or from public or private research centers.

L'archive ouverte pluridisciplinaire **HAL**, est destinée au dépôt et à la diffusion de documents scientifiques de niveau recherche, publiés ou non, émanant des établissements d'enseignement et de recherche français ou étrangers, des laboratoires publics ou privés.

CHEMFIRE: A ZONE MODEL FOR PREDICTING CHEMICAL EFFECTS OF POOL FIRE IN A SINGLE FORCED VENTILATION ENCLOSURE

S. Brohez*, C. Delvosalle* and G. Marlair**
sylvain.brohez@fpms.ac.be
***Faculté Polytechnique de Mons, Belgium**
****Institut National de l'Environnement Industriel et des Risques, France**

Abstract
Zone models have been developed since the early 60s for the prediction of fire parameters such as smoke temperature, smoke filling and movement in multi-compartment buildings. Unfortunately, one major difficulty in current zone models is that heat and chemical species release rates in relation with a given fire source term are usually to be provided as input data. A new zone model for prediction of thermal and chemical effects of pool fire in a forced ventilated enclosure has been developed. The novelty of the approach relies in particular on the provision of three sub-models that are used for reducing the number of input data needed for a given simulation. The burning rate history of liquid pool fire is calculated from a vaporisation sub-model. A solid flame sub-model is used for predicting radiative properties of flame. Yields of chemical species are estimated from a dedicated sub-model of combustion. This zone model has received some validation for use in forced ventilated enclosures only. Promising results have been obtained.

1. Introduction

A large fire in a compartment is often considered as one of the most hazardous accidental event which may affect safety in industries. The fire damages may be thermal or non thermal. For examples, intense radiation produced by large fires may cause serious burn injuries to the staff of the industrial premises and the fire fighters. Moreover, the fire plume may transport a variety of toxic pollutants which can be very dangerous for people, and polluted extinction waters while unconfined may greatly affect the aquatic environment.

Zone models have been developed since the early 60s for predicting fire parameters such as smoke temperature, smoke filling and movement in multi-compartment buildings [1]. In this zone modelling approach, the space within each compartment is generally divided into one or two control volumes [2-4]. Following experimental observations of thermal stratification of gases inside the compartment (pre-flashover fires), two-zone models divide the room gas volume into two distinct and uniform layers: an upper layer of hot gases and a lower layer of air. Inside each of those layers, gas-phase physical parameters such as temperature and species concentrations are assumed to be uniform. On the other hand (post-flashover fires), one-zone models consider a single layer in the compartment, gases inside the compartment are supposed well-mixed. The physical parameters (temperature and composition of gas) of the layers are predicted by solving mass and energy conservation equations on each layer.

Unfortunately, zone models still have important limitations. One major difficulty in current zone models is that heat and chemical species release rates in relation with a given fire source term have usually to be provided as input data. Consequently, there is no feedback interaction between ventilation conditions and these input parameters, which could be assumed unrealistic in many practical cases since ventilation conditions are generally unknown prior to running the simulation. In order to avoid the mentioned drawbacks, a new

zone model has been developed for simulating the behaviour of liquid pool fires in enclosures. The novelty of the approach relies in particular on the provision of three sub-models that are used for reducing the number of input data needed for a given simulation. The burning rate history of liquid pool fire is calculated from a vaporisation sub-model. A solid flame sub-model is used for predicting radiative properties of flame. Yields of chemical species are estimated from a dedicated sub-model of combustion. At present time, this zone model has received some validation for use in forced ventilated enclosures only.

2. Control volumes of the zone model

In the conditions of the experiments conducted for validation purposes of the proposed model (in an enclosure with forced ventilation), fires carried out with low ventilation rates were observed to produce single layer environment in terms of chemical species concentrations [5,6]. Accordingly, in the zone model, the gas phase inside the enclosure is thus supposed well stirred.

Moreover, in classical zone modelling approach, the point source thermal model is considered for the flame, the energy radiated by the flame is specified by the user and is a fraction of the heat release rate (typically 30%). In the development of this zone model, the classical solid flame radiation model initially developed for fire in open space [7] is considered for modelling the flame in the compartment. Accordingly, there are two control volumes: one for the flame and one for the fumes (see fig. 1).

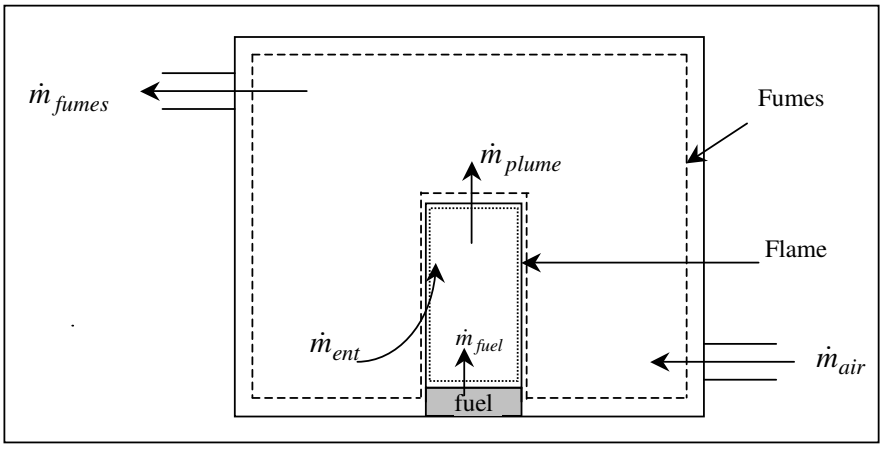


Figure 1. Control volumes selected in zone modelling

3. Vaporisation sub-model

One major difficulty in classical zone models is that mass burning rate (or heat release rate) in relation with a given fire source term is usually to be provided as input data. As this zone fire model is dedicated to simulate liquid pool fires in enclosures, the mass burning rate is predicted from correlation of Zabetakis & Burgess [8] valid in open space:

$$\dot{m}_f'' = 10^{-3} \cdot \frac{\Delta H_{comb}}{\Delta H_{vap}} \qquad (1)$$

where $\dot{m}_f''$ = mass burning rate (kg.m^{-2}.s^{-1}); ΔH_{comb} = heat of combustion ; and ΔH_{vap} = heat of vaporisation at the boiling point of the liquid fuel.

However, in the configuration of the one-zone model, the air entrained into the fire is partially depleted in oxygen. The reduced oxygen concentrations at the base of flame leads to

a reduced mass burning rate [6,9] . The influence of air partly depleted in O_2 on the mass burning rate is introduced additionally by use of the correlation proposed by Peatross & Beyler [6]:

$$\frac{\dot{m}''_f}{\dot{m}''_{f,21\%O_2}} = 0.1\ Y_{O_2}(\%) - 1.1 \tag{2}$$

4. Combustion (chemistry) sub-model

In classical zone models, the yields of chemical species in relation with a given fire source term are usually to be provided as input data. In this zone model, the combustion sub-model is based on the concept of global equivalence ratio Φ [10].

In order to develop the combustion sub-model, experiments were carried out at lab-scale on the Fire Propagation Apparatus operated by INERIS (apparatus in agreement with ASTM E2058) with different mass flow rates of incoming air. For several chemical substances (pyridine, adiponitrile, 1-chlorobutane, thiophène,…), the yields of CO_2, CO, total unburned hydrocarbons, soot, NO, HCN, SO_2, and O_2 were measured as function of the global equivalence ratio [11]. As examples, yields of CO_2 and CO are presented in figure 2, as a function of the equivalence ratio for the solvent pyridine.

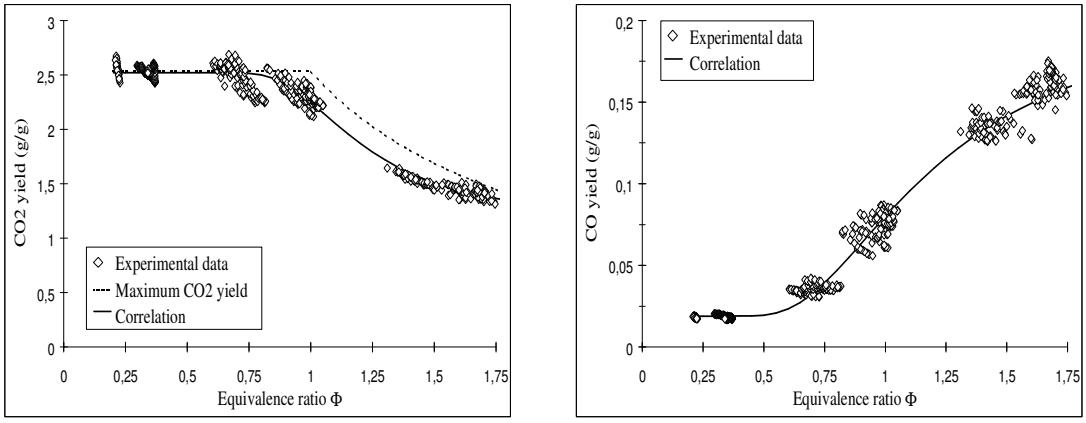


Figure 2. Yields of CO_2 and CO (g/g) as a function of equivalence ratio for pyridine

Following the data processing procedure proposed by Tewarson et al [12], the ventilation controlled fire properties are related to those applying for well-ventilated conditions using the following generalised relationship:

$$\frac{f_i}{f_{i,b.v.}} = 1 + \frac{\alpha}{exp\left(\frac{\Phi}{\beta}\right)^{-\zeta}} \tag{3}$$

where, f_i = fire property valid for any ventilation rate determined by the equivalence ratio value; $f_{i,w.v.}$ = the same fire property applying for well ventilated fires; and α, β and ξ = experimental correlation parameters.

The user has to choose a fuel from a chemical substances database file. This file contains empirical correlation parameters (α, β and ξ) of 8 chemicals species (CO_2, CO, total unburned hydrocarbons, soot, NO, HCN, SO_2, and O_2) as a function of the global equivalence ratio. The yields of N_2 is obtained from the conservation of nitrogen by considering the chemical formulae of the fuel ($C_aH_bO_cN_dX_eS_f$) as well as the NO and the HCN yields:

$$2\,\frac{f_{N_2}}{M_{N_2}} = \frac{d}{M_{comb}} - \frac{f_{NO}}{M_{NO}} - \frac{f_{HCN}}{M_{HCN}} \tag{4}$$

The yields of H_2O is obtained in a similar way as Beyler [13].

It can be pointed out that the database file also contains fuel properties such as heat of vaporisation, specific heat and boiling point. The chemical substances database file today contains fuels such as heptane, adiponitrile, pyridine, TDI, isoproturon, 1-chlorobutane and thiophene.

5. Solid flame sub-model

In the solid flame sub-model, the flame is modelled as an opaque body. The user only specifies the flame diameter. The flame height is given by the well-known Thomas' correlation [14]. Air entrainment into the burning region of pool fire is estimated from correlation established in open space [15].

6. Mass and energy conservation equations

6.1. Fumes control volume

Mass flow rate, chemical species concentrations and temperature of smoke are calculated respectively from mass, chemical species and energy balances on a control volume for gas (smoke) inside the enclosure. The conservation of mass in the fumes control volume leads to the following equation:

$$\dot{m}_{air} + \dot{m}_{pan} - \dot{m}_{fum} - \dot{m}_{ent} = \frac{d\left(\frac{V_{fum}\cdot\ \rho_{fum}}{M_{fum}}\right)}{dt} \tag{5}$$

where $\dot{m}_k$ = molar flow rate of flux k; V_{fum}, ρ_{fum} and M_{fum} are respectively the volume, the density an the molecular weight of fumes.

It is convenient to considered all gaseous species as ideal gases. An ideal gas is any gas that obeys the following ideal gas equation:

$$P\ M = \rho\, R\, T \rightarrow \rho = \frac{PM}{RT} \tag{6}$$

where P = the pressure; and R = the universal gas constant.

As the pressure inside the compartment can be supposed constant [16], then substituting ρ_{fum} in equation 5 by equation (6) leads to the following equation (7) :

$$\dot{m}_{air} + \dot{m}_{pan} - \dot{m}_{fum} - \dot{m}_{ent} = \frac{P}{R}\frac{d\left(\frac{V_{fum}}{T_{fum}}\right)}{dt} \tag{7}$$

The conservation of species i in the fumes leads to the following equation:

$$\dot{m}_{air}\ y_{i,air} + \dot{m}_{pan}\ y_{i,pan} - y_{i,fum}\,(\dot{m}_{fum} + \dot{m}_{ent}) = \frac{P}{R}\frac{d\left(\frac{V_{fum}\cdot y_{i,fum}}{T_{fum}}\right)}{dt} \tag{8}$$

where $y_{i,k}$ = molar fraction of species *i* in flux *k*.

The conservation of energy in the fumes leads to the following equation:

$$\dot{m}_{air}\ h_{air} + \dot{m}_{pan}\ h_{pan} - (\dot{m}_{fum} + \dot{m}_{ent})\,h_{fum} + \dot{q}_{fum} = \frac{P}{R}\frac{d\left(\frac{h_{fum}}{T_{fum}}\right)}{dt} \tag{9}$$

where h_k = molar enthalpy of flux *k* ; and $\dot{q}_{fum}$ = net heat transfer to the fumes (W)

6.2. Flame control volume

Mass flow rate and chemical species concentrations of plume are calculated respectively from mass and chemical species balances on a control volume for flame. It is assumed that time constant of flame is small in comparison with that one of fumes. Hence, a quasi-steady state is assumed for flame (the volume, composition and temperature of flame are assumed to change slowly over the duration of the time step). The conservation of mass in flame control volume leads to the following equation:

$$\dot{m}_{ent} + \dot{m}_{fuel}\sum_{i=1}^{N+1}\left(f_i\frac{M_{fuel}}{M_i}\right) - \dot{m}_{pan} = 0 \tag{10}$$

where $N+1$ = number of species ; and f_i = chemical yields of species *i* (g of *i*.g^{-1} of fuel)

The conservation of species *i* in the flame leads to the following equation:

$$\dot{m}_{ent}\ \ y_{i,fum} + \dot{m}_{fuel} f_i \frac{M_{fuel}}{M_i} - \dot{m}_{pan}\ \ y_{i,pan} = 0 \tag{11}$$

The conservation of energy in the flame leads to the following equation:

$$\dot{m}_{ent}\ \ h_{fum} + \dot{m}_{fuel}\ \ h_{fuel} - \dot{m}_{pan}\ \ h_{pan} - \dot{q}_{flam} = 0 \tag{12}$$

where $\dot{q}_{flam}$ = net heat transfer from the flame (W)

6.3. Finite-difference approximation

The differential equations on the fumes control volume are discretised by a classical finite difference scheme. The second-order accurate central difference formula is used to discretise the first derivatives.

7. Heat transfer sub-model

7.1. Radiation heat transfer

Governing equations

The ceiling, the floor and the vertical walls of the compartment are assumed to be made in the same material and to have the same behaviour (same thermophysical properties and same surface temperature). Consequently, the inside surface of the enclosure forms an unique opaque surface. In addition to the wall surface, the flame is modelled as an opaque body (a surface enveloping the flame has to be considered). The wall surface and the flame surface are modelled as diffuse-grey bodies. The layer of fumes filling the enclosure is an absorbing-emitting medium. Radiative heat transfer between N surfaces in a participating medium is described by the following equation [17]:

$$\sum_{j=1}^{N}\left(\frac{\delta_{kj}}{\varepsilon_j}-F_{k-j}\frac{1-\varepsilon_j}{\varepsilon_j}\tau_{j-k}\right)\dot{q}_j^{''}=\sum_{j=1}^{N}\left(\left(\delta_{jk}-F_{k-j}\,\tau_{j-k}\right)\sigma T_j^4-F_{k-j}\alpha_{j-k}\sigma T_{fum}^4\right) \tag{13}$$

where $\dot{q}_j^{''}$ = net radiative heat flux leaving surface j ; δ_{kj} = the Kronecker symbol ; ε_j = emissivity of surface j ; F_{kj} = view factor from surface k to surface j ; τ_{j-k} = fraction of the radiation from surface j to surface k transmitted through the gas ; α_{j-k} = fraction of the radiation from surface j to surface k absorbed by the fumes ; T_j = temperature of surface j ; and T_{fum} = temperature of fumes

As the flame is opaque, the fuel surface only see the surface of the flame base. The flame surface is divided into two surfaces (of same temperature and same emissivity) S_{flam_1} and S_{flam_2} :

$$S_{flam_1}=S_{fuel}+\pi D H \qquad\qquad S_{flam_2}=S_{fuel} \tag{14}$$

The net radiation equation (13) applied to the wall surface (S_w) and the flame surface (S_{flam_1}) leads the following equations:

$$\begin{aligned}&\left(\frac{1}{\varepsilon_w}-F_{w-w}\frac{1-\varepsilon_w}{\varepsilon_w}\tau_{w-w}\right)\dot{q}_{rad,wall}^{''}-F_{w-flam_1}\frac{1-\varepsilon_{flam}}{\varepsilon_{flam}}\dot{q}_{rad,flam_1}^{''}\\&=\left(1-F_{w-w}\tau_{w-w}\right)\sigma T_{wall}^4-F_{w-flam_1}\,\tau_{flam_1-w}\,\sigma T_{flam}^4-\varepsilon_{fum}\sigma T_{fum}^4\end{aligned} \tag{15}$$

$$\begin{aligned}&-F_{flam_1-w}\frac{1-\varepsilon_w}{\varepsilon_w}\tau_{w-flam_1}\,\dot{q}_{rad,wall}^{''}+\frac{1}{\varepsilon_{flam}}\dot{q}_{rad,flam_1}^{''}\\&=-F_{flam_1-w}\,\tau_{w-flam_1}\,\sigma T_{wall}^4+\sigma T_{flam}^4-\varepsilon_{fum}\,\sigma T_{fum}^4\end{aligned} \tag{16}$$

A solvable system of two equations (15 and 16) with two unknowns ($\dot{q}_{rad,wall}^{''}$ and $\dot{q}_{rad,flam_1}^{''}$) is obtained. The net radiation equation (13) applied to the fuel surface (S_{fuel}) and flame surface (S_{flam_2}) leads the following equations:

$$\dot{q}''_{rad,flam_2} = -\dot{q}''_{rad,fuel} = \frac{\sigma T_{flam}^4 - \sigma T_{fuel}^4}{\frac{1}{\varepsilon_{flam}} + \frac{1}{\varepsilon_{fuel}} - 1} \tag{17}$$

The net radiative heat flux leaving flame surface $\dot{q}_{rad,flam}$ is given by the following equation:

$$\dot{q}_{rad,flam} = S_{flam1}\ \dot{q}''_{rad,flam1} + S_{flam_2}\ \dot{q}''_{rad,flam2} \tag{18}$$

View factors

The view factor F_{kj} is defined as the fraction of radiant energy leaving surface k and that is incident to surface j. The view factor F_{flam_1-w} from surface S_{flam_1} to wall surface is equal to unity.

From the reciprocity relation, we can obtain F_{w-flam_1} :

$$S_{walls}\ F_{w-flam_1} = S_{flam_1}\ F_{flam_1-w} \tag{19}$$

Finally, as the wall surface and the flame surface S_{flam_1} form an enclosure, we have the following equation for F_{w-w} (all the fractions of energy leaving wall surfaces and reaching the surfaces of the enclosure must total to unity):

$$F_{w-flam_1} + F_{w-w} = 1 \tag{20}$$

Gas emissivity

Radiation properties depend on several parameters such as gas properties (temperature, pressure, nature of constituents) wavelength and geometry of the gas volume [17,18]. For engineering applications, the diffuse-grey assumption is used for flame surface and fumes; hence, mean radiation properties (integrated over the whole spectrum of wavelengths) are used. Moreover, the notion of equivalent mean beam length is used for the flame and the fumes in order to simplify the analysis:

$$L_{eq,flame} = \frac{3.6\,V_{flame}}{S_{flame}} \qquad L_{eq,fumes} = \frac{3.6\,V_{fumes}}{S_{fumes}} \tag{21}$$

Emissivities of smoke and flame are calculated by taking into account main contributing emissivities of CO_2, H_2O and soot [19]:

$$\varepsilon = \varepsilon_g + \varepsilon_s - \varepsilon_g \varepsilon_s \qquad \varepsilon_g = \varepsilon_{CO_2} + \varepsilon_{H_2O} - \Delta\varepsilon \tag{22}$$

The emissivities of CO_2 and H_2O are calculated using Modak correlations [20]. The emissivity of soot is calculated according to Yuen & Tien [21].

7.2. Convection heat transfer

Convection heat transfer is described by the following equation:

$$\dot{q}''_{conv,walls} = h(T_{walls} - T_{gaz}) \tag{23}$$

where, h = Mean convection coefficient to walls ($W.m^{-2}.K^{-1}$)

The convective heat transfer coefficient can be obtained from empirical correlations for natural convection based on Nusselt, Grashof and Prandtl numbers [22]:

$$Nu = F(Gr, Pr) \tag{24}$$

The convective heat transfer coefficients are approximately the same for vertical and horizontal walls. In order to simplify the procedure, the same weighted average value is taken for the vertical and horizontal walls.

$$h_{averaged} = \frac{4\,h_{vertical\ walls} + h_{ceiling} + h_{floor}}{6} \tag{25}$$

7.3. Conduction heat transfer

In radiation and convection heat transfer equations, the wall temperature T_{wall} is still an unknown. This temperature is calculated from the one-dimensional heat conduction model [23]:

$$\rho\, c_p \frac{\partial T(t,x)}{\partial t} = \lambda \frac{\partial^2 T(t,x)}{\partial x^2} \tag{26}$$

where, ρ, c_p and λ = respectively the density, the heat capacity and the conductivity of the wall material ; x = space coordinate ; $T(t,x)$ = temperature profile in the wall at time t.

The user may choose the nature of the compartment surfaces from a thermophysical properties database file (containing values of density, heat capacity, conductivity and emissivity of walls).

In order to be coherent with the discretisation of differential equations obtained on the fumes control volume, the Crank-Nicolson finite difference method is applied for discretising the one-dimensional heat equation. Hence, equation 26 at any of the interior nodes (*i=1…M-1*) is discretised as follows (the walls are subdivided into M equal parts of mesh size):

$$-rT_{i-1}^{n+1} + (2+2r)T_i^{n+1} - rT_{i+1}^{n+1} = rT_{i-1}^{n} + (2-2r)T_i^{n} + rT_{i+1}^{n} \tag{27}$$

with, $r = \frac{a\,\Delta t}{(\Delta x)^2}$ and $a = \frac{\lambda}{\rho\, c_p}$

where, T_i^n = temperature of node i at the time level n ; a = material thermal diffusivity

Equation 26 provides M-1 algebraic equations but contains M+1 unknown node temperatures. We need also to consider the two boundary conditions (flux boundary condition for node *x=0* and convection boundary condition for node *x=L*):

$$\text{x=0,} \quad (2+2r)T_0^{n+1} - 2rT_1^{n+1} = (2-2r)T_0^{n} + 2rT_1^{n} + \frac{2\ r\ \Delta x}{\lambda}(\dot{q}_0''(t_n) + \dot{q}_0''(t_{n+1})) \tag{28}$$

$$x=L, \quad -2rT_{M-1}^{n+1} + (2+2r\beta_L)T_M^{n+1} = 2rT_{M-1}^{n} + (2-2r\beta_L)T_M^{n} + 4r\gamma_L \tag{29}$$

with, $\beta_L = 1 + \frac{\Delta x\ h_M}{\lambda}$ and $\gamma_L = \frac{\Delta x\ h_M}{\lambda} T_{air}$

where, $\dot{q}_0''(t_{n+1})$ = net heat flux (W.m^{-2}) applied to the boundary surface $x=0$ at time level t_{n+1} ; h_M = convection heat transfer coefficient at boundary surface $x=L$.

The net heat flux received by the inside surface is composed of convection and radiation heat transfers to the inside walls:

$$\dot{q}_0'' = -\dot{q}_{ray,walls}'' - \dot{q}_{conv,walls}'' \tag{30}$$

Equations 27 to 29 lead to a tridiagonal system of M+1 algebraic equations with M+1 unknown node temperatures T_i^{n+1}. In order to solve this system by the Thomas' algorithm (which is valuable for linear systems), the source term $\dot{q}_0''$ in the boundary equation 28 was linearised by the Newton-Raphson iterative method.

As air temperature inside the compartment can be different of ambient air temperature T_{air}, conduction equations must be solved at time level 0 in order to obtain the initial conditions T(x,0). At time level 0, we can point out that we have a convection boundary condition for node x=0.

8. Validation

Experiments were carried out in a forced ventilation enclosure of 80 m^3 (at INERIS) with pyridine pool fires. The compartment is approximately 4.9 m wide by 4 m deep by 4 m high (figure 3). The walls, floor and ceiling consist of 20 mm thick concrete. The centre of the inlet opening (0.2 m in diameter) is 0.5 m above the floor. The centre of the exit opening (0.5 m x 0.5 m) is 3.25 m above the floor. Pyridine was placed in a steel pan of 0.564 m diameter. This pan was placed on a load cell in the centre of the floor. A total of five tests with different ventilation conditions were performed (ventilation flow rates were decreased stepwise from 1300 to 280 Nm^3.h^{-1}).

The flow rate of air was measured using a Pitot probe and a thermocouple located inside the inlet duct. Humidity of ambient air was also measured. The flow rate of fumes was measured using a bi-directional probe and a thermocouple located in the exhaust duct. Molar fractions of O_2, CO_2, CO and NO in the exhaust duct were measured. Molar fraction of THC and generation of HCN in the exhaust duct were measured using respectively a flame ionisation detector and an automatic titrimeter (a heated sampling line was used). Generation of soot was measured using a gravimetric soot measuring device. Molar fraction of O_2 inside the compartment (50 cm from floor - North tree) was also measured.

There were four thermocouple trees to measure gas temperatures inside the compartment. Trees were located in the median plans of the compartment at one meter from the vertical walls. Gas temperatures were measured by Type K thermocouples of 1 mm in diameter [24]. East and west trees contain 2 thermocouples located at 1 m et 2.5 m above the floor. South tree contain 15 thermocouples spaced 25 cm apart beginning 25 cm above the floor. North tree contain 8 thermocouples spaced 50 cm apart beginning 25 cm above the floor.

In terms of input data, the model basically requires the knowledge of the mass of fuel, the pool fire (pan) area, the mass flow rate, the temperature and humidity of incoming air and the compartment geometry in relation with a given scenario. In a final step of the initial procedure, the user also chooses the fuel and the nature of compartment surfaces from two database files.

The flame temperature predicted by the model was strongly underestimated. Indeed, the conservation of energy for flame leads to temperature of about 300°C, which is typical of plume temperature. In order to solve this problem, flame temperature must be introduced as

an input data. In a forthcoming development, this parameter will be calculated from the conservation of energy on a new control volume, the persistent region of flame.

Figure 4 presents the comparisons for fuel burning rate (for the five tests, in steady state conditions) between the experimental results and the model predictions. The smaller is the ventilation rate, the smaller is the fuel burning rate because of vitiation of air entrained into the base of the flame. The model leads to fairly good predictions of fuel burning rate.

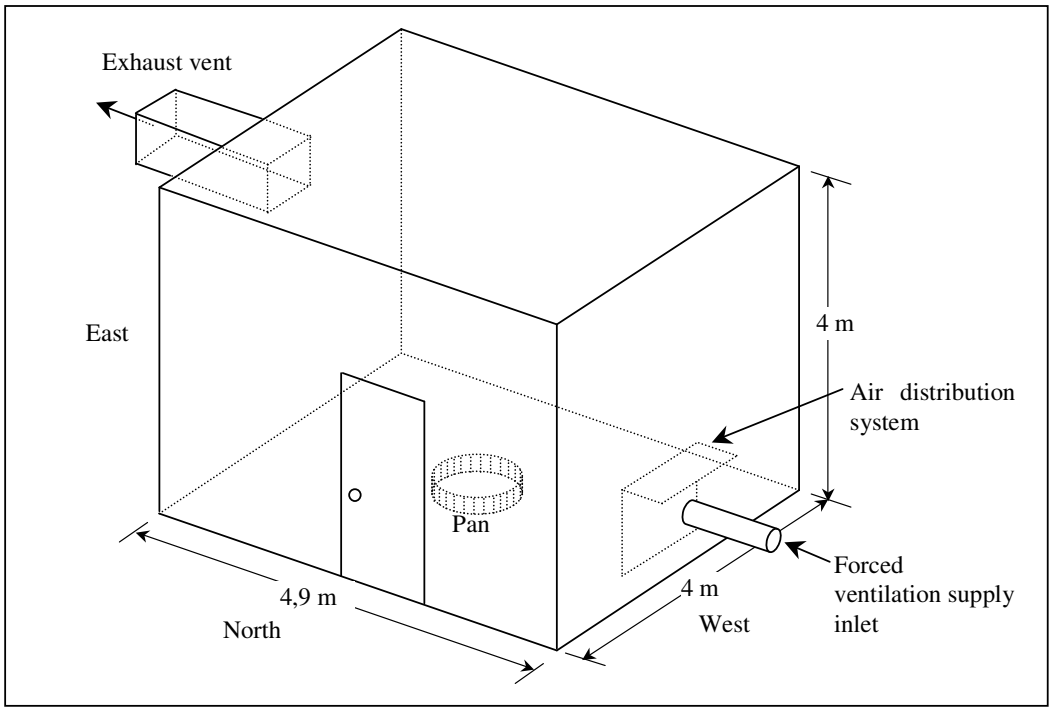


Figure 3. Schematic of the INERIS forced ventilated fire compartment

In order to analyse more finely the combustion sub-model (comparisons of chemical effects between the experiments and the model predictions), the actual fuel burning rate was also fixed as input data (the yields of combustion products depend on the value of the equivalence ratio which depends on the fuel burning rate). The paper now discusses the results obtained for the experiment carried out with an air ventilation rate of 280 $Nm^3.h^{-1}$ (the least ventilated test configuration). In this configuration, we can point out that the equivalence ratio was about 0.55.

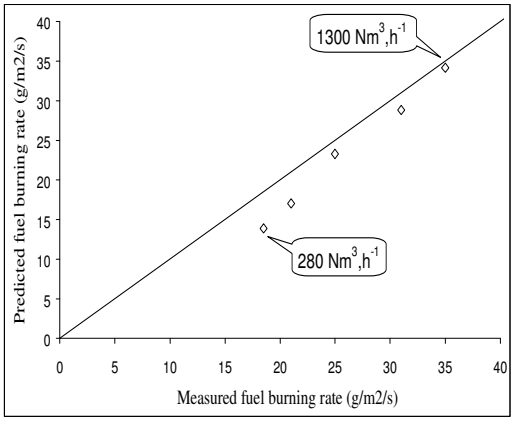


Figure 4 . Comparison of measured and predicted fuel burning rate in steady state conditions

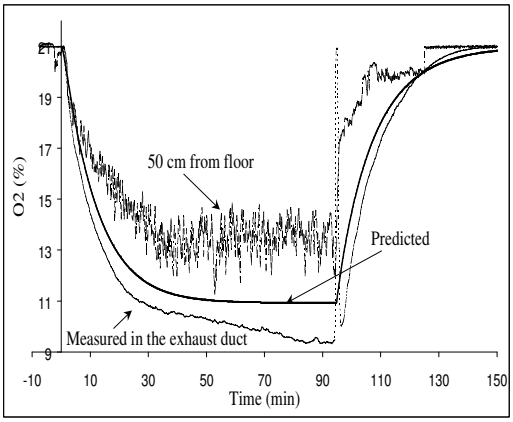


Figure 5 . Comparison of measured and predicted O_2 concentrations (ventilation rate =280 $Nm^3.h^{-1}$)

For concentrations of O_2 and CO_2 (see fig. 5 and 6), there is a good agreement between the predicted and measured values. Prediction of concentrations of O_2 and CO_2 are respectively overestimated and underestimated by 10%. This difference could be the consequence of an overestimation of the measured ventilation rate of the compartment.

For concentration of CO (see fig. 7), there is a strong difference between calculated and measured values (zone model version 1). The concentration of CO is underestimated by a factor of about 2. We can point out that molar fraction of oxygen at the flame base has an effect on the CO yield [10,25]. In our case, molar fraction of oxygen at the flame base is equal to about 13%. Hence, in the sub-model of combustion, we have introduced the correlation of Mulholland et al [25] in order to take into account the influence of oxygen concentration on the CO yield. As can be seen, there is now a good prediction of CO concentration (zone model version 2).

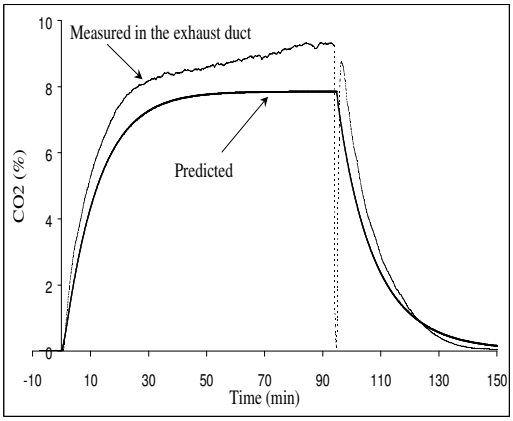


Figure 6. Comparison of measured and predicted CO_2 concentrations (ventilation rate =280 $Nm^3.h^{-1}$)

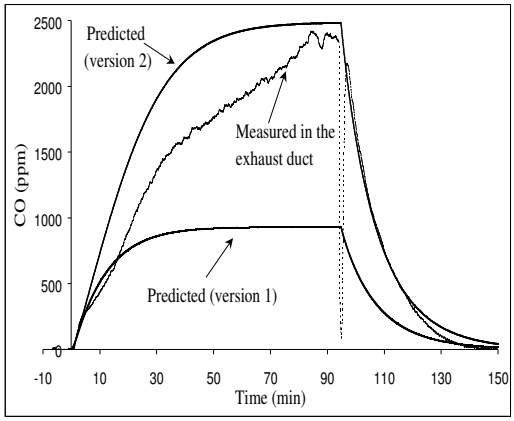


Figure 7. Comparison of measured and predicted CO concentrations (ventilation rate =280 $Nm^3.h^{-1}$)

9. Conclusion

A new zone model for predicting thermal and chemical effects of pool fire in a forced ventilation enclosure has been developed. The main differences between this model and classical zone models rely on the development of three sub-models that are used for reducing the number of input data needed for a given scenario. The burning rate history of liquid pool fire is calculated from a vaporisation sub-model. A solid flame sub-model has been developed for predicting radiative properties of flame. Yields of chemical species are estimated from a dedicated sub-model of combustion which is based on experimental results obtained at lab-scale and introduced in a fuel database. This zone model has received some validation for use in forced ventilation enclosures. Promising results have been obtained. For a more general point of view, this is very encouraging as fire safety engineering techniques based on this type of approach are clearly needed for addressing some important safety issues in enclosures such as warehouses.

References

[1] Janssens M.L. Room Fires Models. General. In *Heat Release in Fires,* edited by V. Babrauskas and S.J. Grayson, Chapter 6(a), 113-157 (1992)

[2] Cox G. Compartment Fire Modelling. In *Combustion Fundamentals of Fire,* edited by Cox G., Academic Press, Chapter 6, 329-404 (1995)

[3] Jones W.W., Forney G.P., Peacock R.D. and Reneke P.A. A Technical Reference for CFAST: An Engineering Tool for Estimating Fire and Smoke Transport. Technical Note 1431, National Institute of Standards and Technology, Gaithersburg, MD (2000)

[4] Quintiere J.G. Fundamentals of Enclosure Fire Zone Models. *Journal of Fire Protection*

Eng., Vol. 1 (3), 99-119 (1989)
[5] Backovsky J., Foote K.L. and Alvares N.J. Temperature Profiles in Forced-Ventilation Enclosure Fires. *Proc. Fire Safety Science, 2,* 315-324 (1988)
[6] Peatross M.J. and Beyler C.L. Ventilation Effects on Compartment Fire Characterization. Proc. *Fire Safety Science, 5,* 403-414 (1997)
[7] Mudan K.S. Thermal Radiation Hazards from Hydrocarbon Pool Fires. *Prog. Energy and Combustion Science*, vol.10, 59-80 (1984)
[8] Zabetakis M.G. Burgess D.S. Research in Hazards Associated with the production and handling of liquid hydrogen, US bureau of Mines Report, RI 5707 (1961)
[9] Nikitin Y.V. Variations of Mass Combustion Rate with Oxygen Concentrations and Gas Pressure of a Milieu. *Journal of Fire Sciences*, v.16, 458-467 (1998)
[10] Pitts W.M. The Global Equivalence Ratio Concept and the Formation Mechanisms of Carbon Monoxide in Enclosures Fires. *Prog. Energy Combust. Sci*., 21, 197- 237 (1995)
[11] Brohez S. Marlair G. and Delvosalle C. Fire calorimetry relying on the use of the Fire Propagation Apparatus. Part 2: burning characterstics of selected chemical substances under fuel rich conditions, *Fire and Materials,* accepted for publication
[12] Tewarson A. Jiang F.H. and Morikawa T. Ventilation-Controlled Combustion of Polymers, *Combustion and Flame*, 95, 151-169 (1993)
[13] Beyler C.L. Major Species Production by Diffusion Flames in a Two-Layer Compartment Fire Environment. *Fire Safety Journal*, 10, 47-56 (1986)
[14] Thomas P.H. The Size of Flames from Natural Fires. *9th Symposium (International) on Combustion*, 844-859 (1963)
[15] Delichatsios M.A. Air Entrainment into Buoyant Jet Flames and Pool Fires, *Combustion and Flame*, 70, 33-46 (1987)
[16] Zukoski E.E. Development of a stratified Ceiling Layer in the Early Stages of a Closed-Room Fires. *Fire and Materials*, 2, 54-62 (1978)
[17] Siegel R. and Howell R.J. The Engineering Treatment of Gas Radiation in Enclosures. Chapter 13, in *Thermal Radiation Heat Transfer*, 3rd Edition, Hemisphere Publishing Corporation, 597-681 (1992)
[18] Tien C.L., Lee K.Y. and Stretton A.J. Radiation Heat Transfer. *The SFPE Handbook of Fire Protection Engineering*, Sect 1, Chap 4, 1-65 to 1-79. NFPA Press, Quincy, (1995)
[19] Tien C.L. and Lee K.Y. Flame Radiation. *Prog. Energy Combust. Sci*., 8, 41-59 (1982)
[20] Modak A. Radiation from Products of Combustion. *Fire Research*, 1, 339-361 (1978)
[21] Yuen W.W and Tien C.L. A Simple Calculation Scheme for the Luminous-Flame Emissivity. *Proc. Comb. Inst.*, 16, 1481-1487 (1976)
[22] Atreya A. Convection Heat Transfer. *SFPE Handbook of Fire Protection Engineering*, Sect 1, Chap 3, 1-39 to 1-64. NFPA Press, Quincy, MA (1995)
[23] Özisik M.N. One Dimensional Parabolic System. Chapt 5, in *Finite Difference Methods in Heat Transfer*, CRC Press, 99-149 (1994)
[24] Brohez S. Delvosalle C. and Marlair G. A two-thermocouples probe for radiation corrections of measured temperatures in compartment fires, *Fire Safety Journal*, 39, 399-411 (2004)
[25] Mulholland G., Janssens M., Yusa S., Twilley W. and Babrauskas V. The Effect of Oxygen Concentration on CO and Smoke Produced by Flames. *Proc. Fire Safety Science*, 3, 585-594 (1991)